Canadian Aeronautics and Space Journal, Vol. 11, No. 9, Nov. 1965, pp. 329–333.

[8] Brownlee, W. G. and Roberts, A. K., "Investigations of Nonlinear Axial Combustion Instability in Solid Propellant Rocket Motors," AIAA Paper 63-474, Cambridge, Mass., 1963.

[9] Roberts, A. K., Brownlee, W. G., and Jackson, F., "Combustion Instability and the Design of Solid Propellant Rocket Motors," *Canadian Aeronautics and Space Journal*, Vol. 16, No. 1, Jan. 1970, pp. 21–27.

[10] Dickinson, L. A., Capener, E. L., and Kier, R. J., "Propellant Deflagration Control: A Method for Suppressing Unstable Combustion," *Chemical Engineering Progress Symposium Series*, No. 61, Vol. 62, 1966, pp. 63–69.

[11] Capener, E. L., Dickinson, L. A., and Kier, R. J., "Driving Processes of Finite-Amplitude Axial Mode Instability in Solid-Propellant Rockets," *AIAA Journal*, Vol. 5, No. 5, May 1967, pp. 938–945.

JANUARY 1971 AIAA JOURNAL VOL. 9, NO. 1

A Comparison of Analysis and Experiment for Solid-Propellant Combustion Instability

M. W. Beckstead* and F. E. C. Culick†
Naval Weapons Center, China Lake, Calif.

Combustion instability data obtained with the same propellants utilizing a T-burner and an L^*-burner are presented and compared. Analyses for these burners are combined directly with results of transient analyses of the combustion. The form of the combustion analyses contains two parameters and by the proper combination of the various analyses, these two parameters can be evaluated directly in terms of the experimental variables. The results indicate the parameter values are not consistent nor necessarily realistic. It appears that the theoretical models of transient combustion result in a general, qualitative agreement with experimental data, but that extensive revisions in these models will be necessary in order to obtain quantitative agreement.

Nomenclature

a = average speed of sound
A = parameter in the response function, $A = (1 - T_i/\bar{T}_s) \times (E_s/R_0\bar{T}_s)$
A_b = admittance function defined in Eq. (16)
B = parameter in the response function, Eq. (1)
c^* = characteristic velocity, $c^* = pS_t/(\text{total mass flow})$
E_s = activation energy for surface pyrolysis
h = function defined by Eq. (14)
h_1,h_2 = functions defined by Eqs. (8e), (8f)
k = wave number, $k = (\omega - i\alpha)/a$
k_l = wave number for classical acoustic mode, $k_l = l\pi/L$
L = length of T-burner
L^* = characteristic length, $L^* = V/S_t$
m = mass flux (mass/time-area)
M_b = Mach number at the burning surface
n = index in linear burning rate law, $r \sim p^n$
n_s = index in surface pyrolysis law, $m \sim p^{n_s} \exp(E_s/R_0T_s)$
p = pressure
r = linear burning rate
R = response function, $R = R_r + iR_i$
R_0 = gas constant
$\mathcal{R}$ = universal gas constant
S_b = area of burning surface
S_c = cross-section area of T-burner
S_t = area of nozzle throat
t = time
T = temperature
T_i = initial temperature of cold propellant
T_s = surface temperature
u = speed of gas parallel to axis in T-burner
u = velocity
V = volume of L^*-burner
z = axial coordinate in T-burner
α = growth constant for acoustic waves
α_g = growth constant, Eq. (23)
α_d = decay constant, Eq. (23)
α_t = thermal diffusivity
α_1,α_2 = constants defined in Eqs. (8a), (8b)
β_1,β_2 = constants defined in Eqs. (8c), (8d)
γ = ratio of specific heats
λ = $\lambda_r + i\lambda_i$ = complex function of Ω, Eqs. (9a), (9b)
ρ = gas density
ρ_p = solid density
τ_b = characteristic time for T-burner, Eq. (30)
τ_c = characteristic time for L^*-burner, Eq. (5)
ω = angular frequency
Ω = dimensionless angular frequency, $\Omega = \alpha_t\omega/\bar{r}^2$
$(\bar{\ })$ = denotes mean value
$(')$ = denotes fluctuation

Received July 10, 1969; revision received June 11, 1970. This research is supported under NASA Work Order 6030.

* Research Chemical Engineer, Aerothermochemistry Division; now Technical Specialist, Hercules, Inc., Magna, Utah. Associate Fellow AIAA.

† Associate Professor, California Institute of Technology, Consultant to Aerothermochemistry Division. Member AIAA.

I. Introduction

In recent years combustion instability of solid propellants has been subjected to various studies, both experimental and theoretical. The experimental programs have led to the development of laboratory combustors in which unstable combustion can be studied under well controlled conditions. The most widely used and probably most versatile of these devices is the T-burner. The L^*-burner is another that has been utilized to a considerable extent recently. The research with these burners has led to experimental methods for the determination of the response of the combustion to an incident pressure perturbation. This same response is the end product of the majority of the theoretical studies. It is the purpose of the present study to compare theoretical predictions with the experimental results from a T-burner and an L^*-burner for the same propellants.

It has been shown recently[1] that virtually all of the existing linear analyses of unstable solid propellant combustion re-

duce to the same form of the response function, i.e.,

$$\frac{r'/\bar{r}}{p'/\bar{p}} = \frac{m'/\bar{m}}{p'/\bar{p}} = R = \frac{nAB}{\lambda + A/\lambda - (1 + A) + AB} \quad (1)$$

where $\lambda = \lambda_r + i\lambda_i$ is a complex function of frequency satisfying the equation $\lambda(\lambda - 1) = i\Omega$. The nondimensional frequency is $\Omega = \alpha_t\omega/\bar{r}^2$; n is the burning rate exponent; and A and B are parameters which will be discussed more in detail later. This common result is a consequence of several basic assumptions: 1) the assumption of a homogeneous solid phase with constant thermal properties, 2) neglect of any pressure dependence of surface reactions, 3) a quasi-static gas phase restricting the analyses to the frequency range in which the gas phase responds much faster than the solid, 4) the assumption that a one-dimensional description is adequate, and 5) neglect of condensed phase reactions.

One of the parameters, $A = (1 - T_i/\bar{T}_s)E_s/R\bar{T}_s$, is characteristic of the solid phase only[1,2]; T_i is the cold propellant temperature, $\bar{T}_s$ is the mean surface temperature, and E_s is the surface activation energy. The other parameter B depends principally on properties of the gas phase. The exact definition of B varies from one analysis to another; see Ref. 1 for a summary of the various definitions of B. In order to interpret experimental data involving unstable combustion, it appears evident that the theoretical response function Eq. (1) should be employed. In the event that this works, then one would have a means of classifying propellants according to the values of the parameters A and B. In order to relate A and B to physical parameters of the propellant or motor, a specific combustion model would have to be singled out and employed.

The experimental data being presented here were obtained in an L^*-burner and a T-burner. These two burners are somewhat independent of each other in that the L^*-burner can only be used to obtain data at low, nonacoustic frequencies and at low pressures. The T-burner is more versatile and provides data over a wider range of frequencies (acoustic mode) and pressures. A discussion and comparison of the two burners can be found in a recent article,[3] which also contains pertinent references to earlier work. The pressure in the T-burner is controlled by venting through a subsonic orifice to a surge tank, and the frequency is determined by the length of the burner. For the data included in the present study the pressure was varied from 100 to 800 psi and the frequency range was 500 to 7000 cps. The L^*-burner contains a sonic nozzle which determines the chamber pressure while the frequency is determined in a complicated manner by the burner L^* and the burning rate of the propellant.

In each burner the pressure is recorded as a function of time, permitting the measurement of the frequency and the growth and decay constant. From these measurements the real part of the response function can be calculated. This has been done with the data from both burners for two propellants, and the results are discussed and compared in Sec. III.

It was mentioned that the purpose of the present paper is to compare these experimental results with the available theoretical predictions. Section II of this paper describes a comprehensive approach for accomplishing this. Briefly, the complex response for each of the burners has been found, using the propellant response function Eq. (1) as a boundary condition. Each of the resulting equations is then separated into real and imaginary parts. This procedure gives two equations for each burner, which can then be solved independently for the parameters A and B in terms of the measurable burner parameters. The typical procedure in the past has been to calculate the real part of the response from data and compare it with the real part of the theoretical response, but with two independent parameters available for fitting the data, a truly objective comparison has not been possible. By taking into account the imaginary part of the response, the extra degree-of-freedom has been eliminated, thus allowing a critical comparison between experiment and the available theories. It is the intent of the authors that by making this more critical comparison, the weaknesses and flaws, whether they be in the theoretical analysis or in the experimental methods, will become more apparent, and the end result will be a better understanding of the phenomenon of combustion instability.

II. Analysis of the Burners for Interpretation of Experimental Results

Since only the pressure is measured in the experiments, some analysis is required to infer the response function. Various approximations are necessary, and these must introduce some errors. But it appears at the present time that such errors are unlikely to be so great as to account for the substantial qualitative discrepancies between the measurements and predictions as discussed in Sec. III.

The computations for the L^*- and T-burners appear to be different, principally because the T-burner oscillates in an acoustic wave mode and the L^*-burner does not. However, in each case the propellant response function represents the chief driving force and one eventually finds two equations involving separately the real and imaginary parts of that function. For the simple two parameter formula of Eq. (1) those two equations are sufficient to determine the quantities A and B. The procedure, then, consists of analysis of the burners followed by a graphical presentation which permits evaluation of A and B directly from the burner measurements.

L^*-Burner

In the L^*-burner, the pressure oscillates in phase throughout the chamber, varying in time but nearly uniform in space. The basis of the calculation is the statement of conservation of mass applied to the gases in the chamber[4]

$$(d/dt)(\rho V) = mS_b - S_t p/c^* \quad (2)$$

(See the Nomenclature for symbol definitions.) It will be assumed that the thermodynamic state of the gases is uniform in the chamber and that the burning is confined to a very thin region. Using the equation of state for a perfect gas to eliminate the density ρ, Eq. (2) becomes

$$\frac{V}{\Re T}\frac{dp}{dt} - \frac{pV}{\Re T^2}\frac{dT}{dt} = mS_b - \frac{S_t p}{c^*} - \frac{p}{\Re T}\frac{dV}{dt} \quad (3)$$

The usual process of linearization ($p = \bar{p} + p'$ etc.) is applied, and one finds

$$\frac{c^*L^*}{\Re T}\frac{d}{dt}\left(\frac{p'}{\bar{p}}\right) - \frac{c^*L^*}{\Re \bar{T}^2}\frac{dT'}{dt} = \frac{m'}{\bar{m}} - \frac{p'}{\bar{p}}$$

Some assumption must be made so that the temperature fluctuations can be related to pressure fluctuations. If the oscillations are sufficiently slow, then the temperature will be nearly uniform and $T' \approx 0$ (the isothermal limit). The other extreme is isentropic behavior

$$T'/\bar{T} \approx [(\gamma - 1)/\gamma]\, p'/\bar{p}$$

In either case, the equation can be put in the form

$$\tau_c(d/dt)(p'/\bar{p}) = (m'/\bar{m}) - p'/\bar{p} \quad (4)$$

where

$$\tau_c = \frac{L^*c^*}{\Re T}\begin{cases}1 \text{ (isothermal)}\\ (1/\gamma) \text{ (isentropic)}\end{cases} \quad (5)$$

Values between these two limits are of course conceivable. For example, there has been interest[5,6] in the possible existence of entropy waves downstream of the flame zone during unsteady combustion of a solid. If such waves are present, the temperature fluctuation not only varies throughout the

chamber, but is also not (locally) in phase with the pressure fluctuations. This possibility will be ignored here; the question is not yet resolved, but rough estimates indicate that the associated corrections in the charts will be small. For harmonic oscillations, $p'/\bar{p} \sim e^{i(\omega - i\alpha)t}$ and $\alpha > 0$ for amplitudes increasing in time. Then with R defined as in Eq. (1), Eq. (4) becomes

$$R - 1 = (\alpha + i\omega)\tau_c \tag{6a}$$

of which the real and imaginary parts are

$$R_r = 1 + \alpha\tau_c \tag{6b}$$

$$R_i = \omega\tau_c \tag{6c}$$

With Eq. (1) used for R, it is merely a matter of manipulation to rewrite these two equations in the form of linear equations for A and AB

$$\alpha_1 A + \beta_1 AB = \Omega h_1 \tag{7a}$$

$$\alpha_2 A + \beta_2 AB = -\Omega h_2 \tag{7b}$$

with the definitions

$$\alpha_1 = h_2(1 - \lambda_r) + h_1\lambda_i \tag{8a}$$

$$\alpha_2 = h_1(1 - \lambda_r) - h_2\lambda_i \tag{8b}$$

$$\beta_1 = (h_2 - n)\lambda_r - h_1\lambda_i \tag{8c}$$

$$\beta_2 = (h_2 - n)\lambda_i + h_1\lambda_r \tag{8d}$$

$$h_1 = \omega\tau_c \tag{8e}$$

$$h_2 = 1 + \alpha\tau_c \tag{8f}$$

If one accounts for the growth of sinusoidal waves ($\alpha \neq 0$), then the expressions for λ_r and λ_i are

$$\lambda_r = \tfrac{1}{2}\left(1 + [1/2^{1/2}]\{[16\,\Omega^2 + (1 - \alpha^*)^2]^{1/2} + (1 - \alpha^*)\}^{1/2}\right) \tag{9a}$$

$$\lambda_i = [1/2(2^{1/2})]\{[16\Omega^2 + (1 - \alpha^*)^2]^{1/2} - (1 - \alpha^*)\}^{1/2} \tag{9b}$$

where α^* stands for the dimensionless quantity $4\alpha_t\alpha/\bar{r}^2$. At this point, the slow growth or decay rate of the waves is properly accounted for everywhere in Eqs. (7a, 7b, 9a, and 9b). However, for $\alpha^* < 0.25$ (which is very much smaller than Ω in the range of interest), numerical values of the response function are less than 1% different from those for $\alpha^* = \alpha = 0$. Hence, α^* can be set equal to zero in λ_i and λ_r. On the other hand, $\alpha\tau_c$ in Eq. (6b) is not negligible (even though α may be small) and this term must be retained.

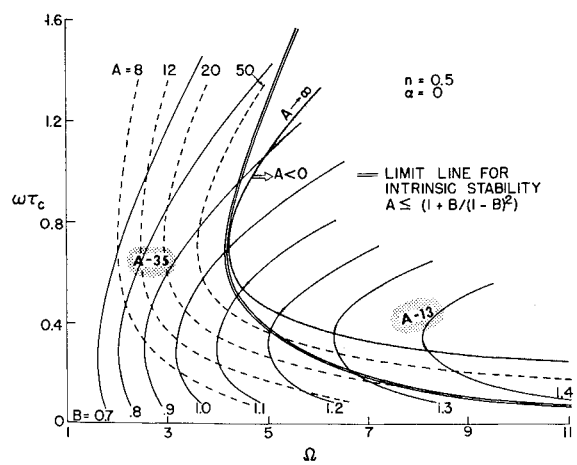

Fig. 1 The L^*-chart for determining the parameters A and B; the regions labeled A-35 and A-13 indicate where the data for those propellants lie.

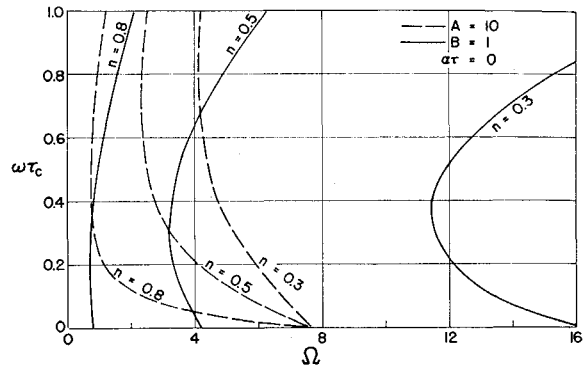

Fig. 2 The L^*-chart with the burning rate exponent as a parameter; only the curves for $A = 10$ and $B = 1$ have been plotted.

Equations (7a) and (7b) can be solved for A and B as functions of Ω, α and $\omega\tau_c$

$$A = \Omega(\beta_1 h_2 + \beta_2 h_1)/(\alpha_1\beta_2 - \alpha_2\beta_1) \tag{10}$$

$$B = -(\alpha_1 h_2 + \alpha_2 h_1)/(\beta_1 h_2 + \beta_2 h_1) \tag{11}$$

The last equations are most conveniently presented as charts for curves of constant A and B with coordinates $\omega\tau_c$ and Ω. The attenuation constant, or rather the combination $\alpha\tau_c$, is treated as a parameter, but since the data will yield results for $\alpha\tau_c = 0$ (Sec. III), only that case is treated here. Figure 1 shows the L^* chart for $\alpha\tau_c = 0$ and $n = 0.5$. If the response function and analysis of the burner are valid, then data from a given propellant, but at different values of L^*, should coincide at a point in the L^* chart thus giving the values of A and B for that propellant. There are two limit lines to be noted. The first (on which A is infinitely large) separates regions of positive and negative values of A. On physical grounds of course, only positive values are acceptable. The position of this line is dependent on both the assumptions used in the analysis of the L^*-burner and on the particular formula used for the response function. The data for A-13 propellant (discussed later) are in the range of values of $(\omega\tau_c, \Omega)$ which results in $A < 0$, indicating an error in one of the analyses or in the assumptions. Accepting the straightforward analysis of the burner and the associated data, the response function (Eq. 1) must be suspected of being an inadequate description of the combustion.

Perhaps the simplest modification that might be considered to improve the response function calculation involves pressure-dependent surface reactions, for which R becomes[7]

$$R = [nAB + n_s(\lambda - 1)]/[\lambda + A/\lambda - (A + 1) + AB] \tag{12}$$

in which n_s is the exponent of the pressure in a modified Arrhenius law, $m \sim p^{n_s}\exp(-E_s/R_0T_s)$. However, Eq. (12) indicates that the limiting line ($A \to \infty$) is virtually unaltered from the simple case [Eq. (1)] and therefore the form of the response function must be suspected of being inadequate.

The other limit line labeled "intrinsic stability" is the locus of A and B for which the denominator of the response function, Eq. (1) or (12), vanishes. If the pair (A, B) lie to the right, then the predicted transient response of the propellant is unstable (see Ref. 1 and other works cited there).

The analysis was also carried out for different values of the burning rate exponent. The results are plotted in Fig. 2 as representative curves for $A = 10$ and $B = 1.0$, each for n equal to 0.3, 0.5 and 0.8. It is apparent that the entire analysis is extremely sensitive to the value of the exponent. In Sec. III it will be pointed out that the data were obtained in a pressure range where n is essentially constant; otherwise, interpretation of the L^* chart would become more complicated.

T-Burner

The analysis for a T-burner is really a special case of the kind of calculation one must perform to study acoustic oscillations in a full-scale rocket chamber. It has recently been shown for two special cases[8] and in general[9] that the results for the L^*-burner can also be extracted as special cases of acoustic calculations. Just as for the L^*-burner, the main result is a complex equation, and both real and imaginary parts should be used. Now, however, the equation is for the eigenvalues for the acoustic modes; the real part gives the attenuation constant and the imaginary part gives the frequency. It is often helpful to regard the problem as analogous to a vibrating string with dissipative, movable supports at the ends.

Following the treatment of Ref. 10 with the mean temperature and pressure uniform in the chamber the equations for one-dimensional velocity and pressure fluctuations are

$$\partial u'/\partial t + (1/\bar{\rho})\partial p'/\partial z = -(\bar{\mathbf{u}}\cdot\nabla\mathbf{u}' + \mathbf{u}'\cdot\nabla\bar{\mathbf{u}})_z$$

$$\partial p'/\partial t + \gamma\bar{p}\,\partial u'/\partial z = -(\bar{\mathbf{u}}\cdot\nabla p' + \gamma p'\nabla\cdot\bar{\mathbf{u}})$$

After differentiation of the first with respect to z and the second with respect to t, these two equations can be combined to give a single second-order equation for p'

$$d^2p'/dz^2 + k^2p' = h \tag{13}$$

where

$$h = i\frac{k}{a}\left[\frac{\bar{u}}{a}\frac{dp'}{dz} + \gamma p'\frac{d\bar{u}}{dz}\right] - \bar{\rho}\frac{d^2}{dz^2}(\bar{u}u') \tag{14}$$

and the assumption of harmonic oscillations has been made, $p' \sim \exp(iakt)$, etc. For convenience in writing, $k = (\omega - i\alpha)/a$. Also, the mean flowfield has been taken to be strictly one-dimensional, so $\bar{u} = \bar{M}_b a$ for $0 \leq z \leq L/2$ and $\bar{u} = -\bar{M}_b a$ for $L/2 < z \leq L$.

Boundary conditions on p' are set in accord with the first of the two original equations

$$dp'/dz = -f = -ika\bar{\rho}u' - \bar{\rho}(d/dz)(\bar{u}u') \tag{15}$$

Now the admittance function is defined conventionally as

$$A_b = (\gamma\bar{p}/a)\,u'/p'$$

with u' positive in the direction away from the surface. Hence, in Eq. (15) one should make the substitution for application at the ends of the burner

$$u' = \pm(a/\gamma\bar{p})A_b p' \tag{16}$$

with the + sign used at $z = 0$ and the − sign at $z = L$, L being the length of the burner.

In order to solve Eq. (13) subject to the boundary condition based on Eq. (15), consider the unperturbed problem for a closed chamber

$$d^2p_l'/dz^2 + k_l^2p_l' = 0 \tag{17}$$

$$dp_l'/dz = 0 \quad (z = 0,L) \tag{18}$$

for which

$$p_l' = \cos(k_l z) \tag{19a}$$

$$k_l = l\pi/L \tag{19b}$$

Now multiply Eq. (13) by (p'_l), Eq. (17) by p', subtract, and integrate over $0 \leq z \leq L$ to obtain

$$(k^2 - k_l^2)\int_0^L p'p_l'dz + \int_0^L\left[p_l'\frac{d^2p'}{dz^2} - p'\frac{d^2p_l'}{dz^2}\right]\times dz = \int_0^L p_l'h dz$$

The second integral can be integrated by parts, and after use of Eq. (15) one has

$$k^2 = k_l^2 + \frac{1}{E_l^2}\left\{\int_0^L hp'_l dz + [fp'_l]\int_0^L\right\} \tag{20}$$

where

$$E_l^2 = \int_0^L p'p_l'dz$$

This is a perturbation calculation, and to find k^2 to first order in the Mach number M_b, it is adequate to substitute the classical values for p' and u' everywhere in the right hand side of Eq. (20). Thus, $p' \cong p_l'$ and $u' \cong (i/\bar{\rho}ak_l)dp_l'/dz$. After all the integrations are done, and proper account is taken of the sign of $\bar{u}$, the result is

$$k^2 = k_l^2 - (4ik_l/L)(A_b + M_b) \tag{21}$$

This is the equation for the complex eigenvalue corresponding to Eq. (6) for the L^*-burner. Note that for $p' = p_l' = \cos k_l z$, $E_l = L/2$ when $l \neq 0$.

Since $\alpha/\omega \ll 1$ for these lightly damped systems, Eq. (21) can be split into real and imaginary parts

$$(\omega L/a)^2 = (l\pi)^2 + 4(\omega L/a)A_b^{(i)} \tag{22}$$

$$\alpha_g L/a = 2[A_b^{(r)} + M_b] - \alpha_d L/a \tag{23}$$

In Eq. (23) $\alpha_d > 0$ represents the attenuation constant associated with dissipative effects other than the mean flow and $\alpha_g > 0$ represents the (measured) growth constant for the growth of acoustic energy during burning. The influence of the mean flow is entirely in the term $2M_b$, except that the effect of a vent does not appear. The last result is a consequence of assuming the vent to be at the center of the chamber where $p' \approx 0$; in such a circumstance, neither can wave energy (proportional to p'^2) be carried away by the flow, nor can work be done on or by the waves.

It has been assumed in the preceding calculation that the speed of sound is uniform in the chamber. Owing to heat losses, this is not true, and the necessary correction may be large. An approximate means of including this refinement may be found in Appendix A of Ref. 3 and Appendix B of Ref. 11.

If the propellant does not fill the head end of the chamber and has burning area S_b, then Eqs. (22) and (23) are replaced by

$$(\omega L/a)^2 = (l\pi)^2 + 4(\omega L/a)(S_b/S_c)A_b^{(i)} \tag{24}$$

$$\alpha_g L/a = 2(S_b/S_c)[A_b^{(r)} + M_b] - \alpha_d L/a \tag{25}$$

The definition of the admittance function gives a relation between A_b and R, for since $m = \bar{m} + m' = (\bar{\rho}\bar{u}) + (\rho u)'$, one has $m'/\bar{m} = \rho'/\bar{\rho} + u'/\bar{u}$ and

$$A_b = \frac{\gamma\bar{p}}{a}\frac{\bar{u}}{p'}\left(\frac{m'}{\bar{m}} - \frac{\rho'}{\bar{\rho}}\right) = \gamma M_b\left(\frac{m'/\bar{m}}{p'/\bar{p}} - \frac{\rho'/\bar{\rho}}{p'/\bar{p}}\right)$$

Note that all properties and velocities are evaluated at the (ill-defined) interface between the chamber and the region of burning; hence $\bar{u}/a$ is in fact M_b. If the waves are assumed to be isentropic at this interface, then $p'/\bar{p} = \gamma(\rho'/\bar{\rho})$ and

$$A_b = \gamma M_b R - M_b \tag{26}$$

The basic Eqs. (24) and (25) become

$$R_r = (S_c/S_b)(1/2\gamma M_b)(\alpha L/a) \tag{27}$$

$$R_i = (S_c/S_b)(1/2\gamma M_b)(1/2l\pi)[(\omega\tau_b)^2 - (l\pi)^2] \tag{28}$$

which should be compared with Eqs. (6b) and (6c) for the L^*-burner. For convenience, the definitions

$$\alpha = \alpha_g + \alpha_d \tag{29}$$

$$\tau_b = L/a \tag{30}$$

have been introduced. Note also that $\gamma M_b = \rho_p r a/\bar{p}$ has been used.

Equation (28) shows that the T-burner operates under conditions when the frequency is not very different from the classical value for a closed tube, since $(\omega\tau_b)^2$ differs from $(l\pi)^2$ by a term of the order of M_b, a very small number. Hence, as an approximation, one can write

$$(\omega\tau_b)^2 - (l\pi)^2 = (\omega\tau_b - l\pi)(\omega\tau_b + l\pi) = 2l\pi(\omega\tau_b - l\pi)$$

and Eq. (28) becomes

$$R_i = (S_c/S_b)(1/2\gamma M_b)(\omega\tau_b - l\pi) \tag{31}$$

Obviously, Eqs. (27) and (28) lead to a chart in the same way that Eqs. (6b) and (6c) did. The solutions for A and B are Eqs. (10) and (11) but with

$$h_1 = \frac{S_c}{S_b}\frac{1}{4\gamma M_b l\pi}[(\omega\tau_b)^2 - (l\pi)^2] \cong \frac{S_c}{S_b}\frac{1}{2\gamma M_b}(\omega\tau_b - l\pi) \tag{32}$$

$$h_2 = (S_c/S_b)(1/2\gamma M_b)\,\alpha L/a \tag{33}$$

The analysis of the T-burner has been covered here in detail mainly because previous discussions have treated only the real part of the eigenvalue, Eq. (27). In that case, one would apparently have two parameters (A and B) and a single equation. This, for example, is the basis for the comparison of Eq. (12) with data for JPN given in Ref. 7. It is clear, however, that such a procedure ignores the important feature that the response function is complex—the phase as well as the magnitude must be considered.

There is an interesting difference between these results for the L^*- and T-burners. For the L^*-burner, a dominant quantity is $\omega\tau_c$, the ratio of the chamber characteristic time to the period of the wave. The corresponding quantity for the T-burner, cf., Eqs. (8e) and (33), is the dimensionless combination of attenuation constants. The oscillation frequency in an L^*-burner is determined essentially by the real part of the response; according to Eq. (6b) it is the frequency at which the real part is $1 + \alpha\tau_c$. Then $\omega\tau_c$ is equal to the imaginary part of R at that frequency.

On the other hand, the frequency of oscillation in a T-burner is (ideally) very close to the value $l\pi a/L$ for a tube with rigid ends. This can be seen from Eq. (28). The Mach number M_b is of the order of 10^{-3} and for expected values of $R_i \approx 1$–10 [e.g., if Eq. (1) is used] then $\omega\tau_b \approx l\pi$. Measured values are generally lower than expected, probably because the temperature, and hence the speed of sound, is lower than that predicted on the basis of adiabatic burning. The attenuation constant α is then determined by the real part according to Eq. (27).

There are two ways of using these results for a double-ended burner.[11] The first and less widely used at the present time is to vary the area ratio S_c/S_b and make measurements only during burning. The observed values of $\alpha_a L/a$ are plotted against S_b/S_c. According to Eqs. (27) and (29) the slope is $2\gamma M_b R_r \equiv 2\rho_p r a\, R_r/\bar{p}$ and the intercept is $-\alpha_d L/a$. A disadvantage is that several firings are required to obtain a single value of the response. Moreover, the losses, represented by α_d, probably change with S_b/S_c. The imaginary part should be determined by plotting S_b/S_c against $\omega\tau_b$, but the uncertainties in averaging the measured frequencies are so great as to render this step virtually useless at present.

The more common technique is based on measurement of the pressure during burning and after burnout with $S_c = S_b$. In this case the main difficulty is associated with determination of the correct value of α_d, which represents the contributions to the net growth constant resulting from all causes other than the mean flow and the burning. Normally, α_d is identified with the decay constant after burnout, but some care is required (see Sect. III) because the frequency after burnout is different from that during burning.

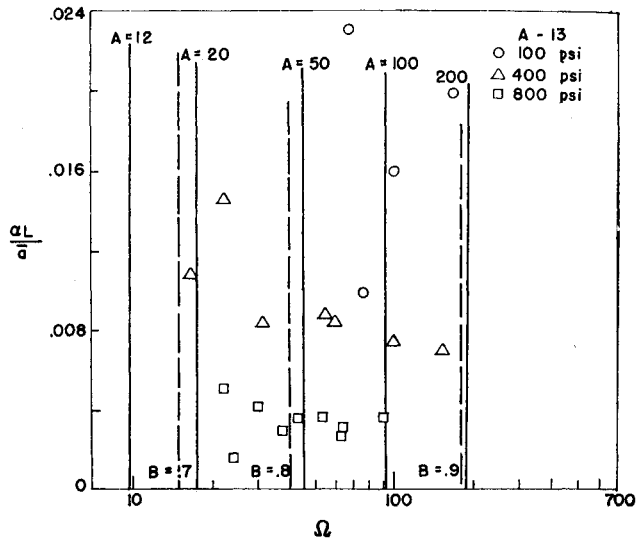

Fig. 3 The T-burner chart for determining the parameters A and B; the data shown are for A-13 at the indicated pressures.

For use with the second approach, a T-chart similar to the L^*-chart can be constructed in the same way. Now, however, the appropriate coordinates are $\alpha L/a$ and Ω, with $\omega\tau_b$ a parameter. Figure 3 shows the results for A-13 propellant with various values of A and B plotted. Similar results are found for A-35 and JPN propellant but are not sufficiently different to be included here. As in the L^*-chart, then, both the real and imaginary parts of the response function have been taken into account. For a given propellant (fixed A and B) the data should lie on vertical lines if the response function and analysis of the T-burner are correct. There are serious qualitative differences between the data and these calculations.

The unanticipated result that lines of constant A and B are vertical (i.e., A and B are functions of Ω only when presented in this way) can be clarified as follows. It has already been noted that the T-burner oscillates at a frequency nearly equal to L/a so $\omega\tau_b \simeq \pi$ at all times in the first mode. If one sets $\omega\tau_b$ exactly equal to π (i.e., $h_1 = 0$) in the formulas (6a) and (6b), one finds easily $A = \Omega\lambda_r/\lambda_i$ and $B = (1 - N)^{-1}(\lambda_r - 1)/\lambda_r$ where $N = 2n\gamma M_b \alpha L/a \ll 1$ because M_b is so small. Hence, lines of constant A and B are essentially functions of frequency only. If $\omega\tau_b \neq \pi$, the lines are affected only slightly (in fact, by changes of order M_b). It must be emphasized that this procedure indeed accounts for non-zero values of R_i; the approximation $\omega\tau_b = l\pi$ has been made only later in the calculation. If R (and in particular R_i) should be a different function of A and B, or should contain additional parameters, then the lines of constant A and B will not in general be vertical in the $(\alpha L/a, \Omega)$ plane. This is an important conclusion which will be referred to later.

III. Comparison of Response Functions

Two different propellant compositions were chosen to provide data for the study, A-13 and A-35. The A-13 propellant contains 76% AP (mean particle size, 90μ) and 24% PBAN binder with an epoxy curative. A-35 contains 75% AP (same size distribution as that used in A-13) and 25% of an Estane type of polyurethane binder. Both of these propellants have been tested extensively at the Naval Weapons Center (some of the T-burner data were obtained under the direction of M. M. Ibiricu[12]) and A-13 has also been used as a

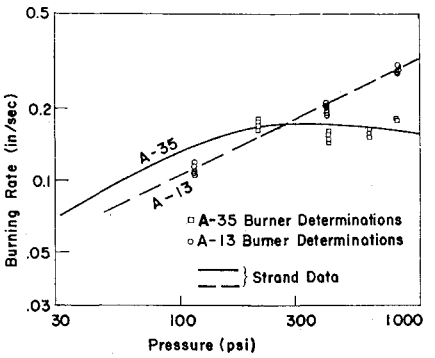

Fig. 4 Burning rate data for A-13 and A-35 propellants.

reference propellant by the ICRPG T-Burner Committee.[11] A comparison of the burning rates of the two propellants is presented in Fig. 4. A-13 has a uniform slope over a wide range of pressures. T-Burner data were obtained at 100, 400 and 800 psi while L^*-burner data were obtained below 200 psi only. For A-35, which has a plateau in the burning rate, T-burner data were obtained at 200, 300, 400 and 800 psi, but again, the L^* data were obtained only at pressures below 200 psi.

Utilizing the analyses discussed the real part of the response can be evaluated from the data obtained in the two burners and correlated with the nondimensional frequency in order to make a direct comparison with Eq. (1). In the case of the L^*-burner the calculation is almost trivial, see Eq. (6b). The growth constant is measured directly from the pressure-time trace as is the frequency, and the chamber time constant can be evaluated from the burner L^* and steady-state gas properties. In calculating the nondimensional frequency the burning rate was taken as that of strand data for a given pressure.

The calculation of R_r for the T-burner is a well established technique.[11-13] From Eq. (27) and the approximate relation $f = a/2L$ the familiar form for calculating R_r from the experimental data is obtained, i.e.,

$$R_r = (\bar{p}/4\rho_p \bar{r} a)(\alpha_g + \alpha_d/f) \tag{34}$$

The density of the propellant is easily measured and the speed of sound was calculated for each pressure from the theoretical adiabatic flame temperature. The pressure was measured directly and the burning rate was determined for each individual run from the pressure-time traces. The burning rates that were determined in this manner were in good agreement with the strand data. The decay constant in Eq. (34) was determined from the pressure trace immediately after burnout as the oscillations decayed. In evaluating Eq. (34) the frequency occurring during the growth was used, but the growth and decay constants were determined for each individual run. They were not smoothed as has been done by the other investigators.[12,13] This introduces more scatter in the calculated results, but hopefully is less subjective in the data reduction.

Figure 5 is a plot of the real part of the response as a function of the nondimensional frequency for A-13 propellant. The small dots represent the results from the L^*-burner. From previous experience[14] we feel that the spread in the L^* data along the frequency coordinate is mainly due to the data scatter and is not a trend. A theoretical curve, fitting the data, would pass through the data at a nondimensional frequency of about 9 with the general slope of the existing theoretical curve. The T-burner results are represented by the larger symbols, with the different symbols designating the different operating pressures. The solid line in the figure represents calculations based on Eq. (1) with the values of A and B as noted. In comparing the curve with the data it would appear to be impossible to fit both the high and the low frequency data with single values of A and B. Also, a very definite pressure effect is seen in the T-burner data. The T-burner data seem to correlate quite well for a given pressure level (as indicated by the dashed lines); however, according to Eq. (1) there should not be any influence of the mean pressure. This appears only in the nondimensional frequency. If an attempt is made to explain these discrepancies the two most obvious refinements that might be considered within the framework of the models are to include pressure dependent surface reactions, or to consider the parameters A and B as functions of pressure.

By including pressure dependence of surface reactions, the magnitude of the response is increased over the high frequency range, but there is still one curve for all pressures. Therefore, this is not an adequate explanation. So far as the parameters A and B are concerned, it has been reported[15] that the surface temperature varies with pressure. It is contained in the parameter A in all models and is typically in the B parameter also.[2] However, a change in the surface temperature of approximately 200° for the pressure range 100–800 psi would give virtually no change in the magnitude of the response at high frequencies. Mainly, the magnitude at the peak of response is increased, but the rest of the curve is practically unchanged. Thus, the influence of mean pressure observed for the A-13 propellant in Fig. 5 probably cannot be adequately explained within the framework of the present

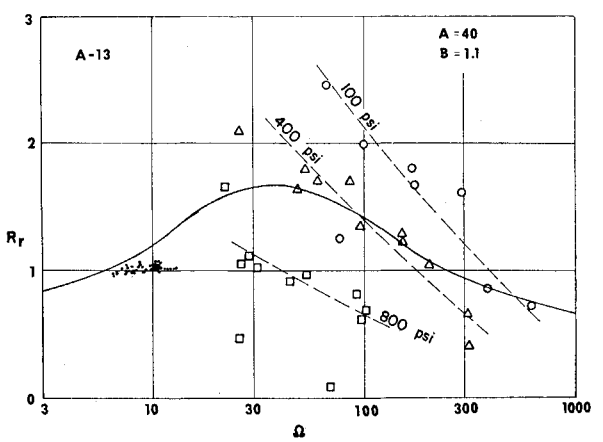

Fig. 5 The real part of the response function vs the nondimensional frequency, $\alpha_t \omega/\bar{r}^2$ for A-13 propellant: the solid curve is calculated from Eq. (1) for the values of A and B shown; the dashed curves represent the T-burner data at the indicated pressures.

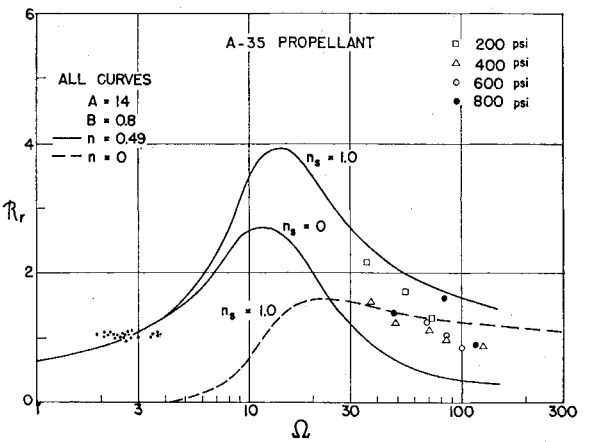

Fig. 6 The real part of the response function vs the nondimensional frequency for A-35 propellant; the curve marked $n_s = 0$ was calculated from Eq. (1) while the curves labeled $n_s = 1.0$ were calculated from Eq. (12) with the term included for pressure dependent surface reactions.

theoretical models by taking into account surface reactions or variations of surface temperature with pressure.

Figure 6 is the corresponding plot for A-35 propellant; the theoretical curves have been calculated using the parameters determined from the L^*-chart (Fig. 1). It was pointed out earlier (see Fig. 4) that the burning rate exponent changes for this propellant from $\sim$0.49 at low pressure where the L^* data were obtained to $\sim$0 above 200 psi where the T-burner data were obtained. This change has been approximated in the theoretical calculations by calculating curves for both values of n. The upper curves of the figure were calculated with $n = 0.49$ while the dashed curve is for $n = 0$ with $n_s = 1.0$. From Eq. (1) it is obvious that for $n = 0$ with $n_s = 0$ the response is zero also. At low frequencies the effect of surface reactions is negligible. The curves for $n = 0.49$ are identical in this region and pass through the L^* data reasonably well. At higher frequencies where the T-burner data were taken, the curve for $n = 0$ is more applicable than the other curves and is seen to approximate the experimental data more closely. Thus, there does seem to be rough agreement between the theoretical analyses and the A-35 data if a first order pressure dependent surface reaction is assumed and the change in burning rate exponent is accounted for as indicated. A possible alternative approach has been treated in Ref. 16, in which it is shown that if condensed phase reactions are included, then a nonzero response may also be found for a plateau or mesa propellant.

Unlike the A-13 data, there is no influence of pressure exhibited by the data taken for A-35 in a T-burner. This appears to be related to the fact that $n = 0$ for A-35 in the range of pressures tested. It also appears that the observed correlation between theory and experiment is related to surface coupled reactions rather than to the purely gas phase reactions. However, the surface-coupled reactions do not improve the correlation of the A-13 data.

IV. Conclusions and Discussion

The approach that has been taken here is based on a combination of the analyses for the L^*- and T-burners with the analytical result for the response function representative of one-dimensional models. The manner in which this comparison is made incorporates both the real and the imaginary parts of the response of the burners as well as for the burning surface. The imaginary part of the response provides an extra degree of freedom which leads to explicit relationships for A and B in terms of the measurable burner parameters. These relations are conveniently represented as plots with lines of constant A and constant B (see Figs. 1–3), and data for two composite propellants have been used to determine the constants. From the L^*-chart one of the propellants (A-35) gave reasonable results ($A = 14$, $B = 0.8$). For the other propellant (A-13) a physically meaningless value of A was found. From the T-burner charts the trends in the data show qualitative disagreement with predictions. The results indicate that the A and B parameters are dependent on frequency, a meaningless conclusion.

The real part of the response calculated from the data as a function of the nondimensional frequency has also been compared directly with the analytical results using what appear to be the most consistent values of A and B. The results for A-13 are definitely not compatible with the analytical results, particularly in the high frequency region. However, this was to be expected from the results of the charts. The results for A-35 appeared to be in agreement with theory, if a first order pressure dependent surface reaction was assumed, and if the change in burning rate exponent was accounted for. The authors feel that the lack of correlation between experiment data (particularly the A-13 data), burner analysis and theoretical analysis is due principally to an inadequate analysis of the transient combustion, although errors in the other areas cannot be ruled out completely.

There are several reasons for doubting the calculation of the combustion analysis response function rather than the analyses of the burners or the accuracy of the data. The acquisition and reduction of the experimental data are relatively straightforward, and although the data could well be in error quantitatively, qualitative errors are probably not of the magnitude being observed here. The analysis of the L^*-burner is very simple; it is not expected to be seriously inaccurate, and yet when the burner and combustion analyses are combined there are gross differences between the analyses and data. This casts suspicion on the combustion analyses. The T-charts are also in poor agreement with the data; however, the T-burner analysis is somewhat more complicated and might be too crude. In this case it is more difficult to locate the possible sources of errors. The third method of comparison was to compare the real part of the theoretical response directly with the data. The agreement was poor, particularly for the propellant with the uniform burning rate exponent. Because the theoretical analysis is common to each method and each method shows poor agreement, it appears that the theoretical analysis of the combustion most probably contains the greatest inaccuracies. Also it does not seem likely that discrepancies as large as those found can be attributed to poor data or to the analyses of the burners.

The most likely sources of error in the models appear to be in the assumptions of quasi-steady behavior in the gas phase and a one-dimensional solid phase. Unreasonable values of A have also been obtained from recent studies with the L^*-burner using bimodal propellants.[17] These studies indicate that the instability is somehow related to the particle size of the oxidizer in the solid phase. This leads one to suspect the assumption of a one-dimensional solid. The observed influence of pressure in the A-13 T-burner data seems to indicate a flaw in the higher frequency portion of the analysis, which of course is related to the quasi-steady assumption. A recent calculation[18] indicates that the first order effect of a small deviation from quasistatic behavior appears in the imaginary but not the real part of the response function. Thus, results for the real part as a function of frequency are unaffected, but the charts (Figs. 1 and 3) are changed. However, no numerical results have been obtained.

One concludes that the theoretical models of transient combustion result in a general, qualitative agreement with the experimental data from laboratory burners. However, in view of the observed differences, it appears that there is ample opportunity for more extensive calculations to improve the major approximations used in the analyses presently available. In particular, the assumptions of quasi-static behavior of the gas phase, and the usual one-dimensional treatment of the solid phase should be considered first.

References

[1] Culick, F. E. C., "A Review of Calculations for Unsteady Burning of a Solid Propellant," *AIAA Journal*, Vol. 6, No. 12, Dec. 1968, pp. 2241–2255.

[2] Denison, M. R. and Baum, E., "A Simplified Model of Unstable Burning in Solid Propellants," *ARS Journal*, Vol. 31, Aug. 1961, pp. 1112–1122.

[3] Beckstead, M. W. et al., "Combustion Instability of Solid Propellants," *Twelfth Symposium (International) on Combustion*, The Combustion Institute, Pittsburgh, Pa., 1969, pp. 203–211.

[4] Beckstead, M. W. and Price, E. W., "Nonacoustic Combustor Instability," *AIAA Journal*, Vol. 5, No. 11, Nov. 1967, pp. 1989–1996.

[5] Waesche, R. H. W., Wenograd, J., and Summerfield, M., "Entropy Wave Observations in Oscillatory Combustion of Solid Propellants: A Progress Report," AIAA Paper 64-154, Palo Alto, Calif., 1964.

[6] Krier, H. et al., "Nonsteady Burning Phenomena of Solid Propellants: Theory and Experiment," *AIAA Journal*, Vol. 6, No. 2, Feb. 1968, pp. 278–285.

[7] Hart, R. W., Farrell, R. A., and Cantrell, R. H., "Theoretical Study of a Solid Propellant Having a Homogeneous Surface Reaction. I. Acoustic Response, Low and Intermediate Fre-

quencies," *Combustion and Flame*, Vol. 10, No. 4, Dec. 1966, pp. 367–380.

[8] Oberg, C. O., "Combustion Instability: The Relationship Between Acoustic and Nonacoustic Instability," *AIAA Journal*, Vol. 6, No. 2, Feb. 1968, pp. 265–271.

[9] Culick, F. E. C., "Some Non-Acoustic Instabilities in Rocket Chambers Are Acoustic," *AIAA Journal*, Vol. 6, No. 7, July 1968, pp. 1421–1423.

[10] Culick, F. E. C., "Acoustic Oscillations in Solid Propellant Rocket Chambers," *Astronautica Acta*, Vol. 12, No. 2, 1966, pp. 113–126.

[11] "T-Burner Manual," CPIA Publ. 191, Nov. 1969, Interagency Chemical Rocket Propulsion Group, Chemical Propulsion Information Agency, Silver Spring, Md.

[12] "Experimental Studies on the Oscillatory Combustion of Solid Propellants," NWC TP 4393, March 1969, Aerothermochemistry Division, Naval Weapons Center, China Lake, Calif.

[13] Horton, M. D., "Testing the Dynamic Stability of Solid Propellants; Techniques and Data," NOTS TP 3610, Aug. 1964, U. S. Naval Ordnance Test Station, China Lake, Calif; also Horton, M. D. and Price, E. W., "Dynamic Characteristics of Solid Propellant Combustion," *Ninth Symposium (International) on Combustion*, Academic Press, New York, 1963, pp. 303–310.

[14] Beckstead, M. W., "Low Frequency Instability: A Comparison of Theory and Experiment," Combustion and Flame, Vol. 12, No. 1, Oct. 1968, pp. 417–426.

[15] Powling, J. and Smith, W. A. W., "The Surface Temperatures of Ammonium Perchlorate Burning at Elevated Pressures," *Tenth Symposium (International) on Combustion*, The Combustion Institute, Pittsburgh, Pa., 1965, pp. 1373–1380.

[16] Culick, F. E. C., "Calculation of the Admittance Function for a Burning Surface," *Astronautica Acta*, Vol. 13, No. 3, May-June 1967, pp. 221–238.

[17] Beckstead, M. W. and Boggs, T. L., "The Effect of Oxidizer Particle Size on Nonacoustic Instability," *4th Combustion Conference, Interagency Chemical Rocket Propulsion Group*, Chemical Propulsion Information Agency, CPIA Publ. No. 162, Vol. 1, Silver Spring, Md., Dec. 1967, pp. 337–346.

[18] Culick, F. E. C., "Some Problems in the Unsteady Burning of Solid Propellants," NWC TP 4668, Feb. 1969, Naval Weapons Center, China Lake, Calif.

JANUARY 1971 AIAA JOURNAL VOL. 9, NO. 1

Gas Phase Reactions near the Solid-Gas Interface of a Deflagrating Double-Base Propellant Strand

C. L. Thompson Jr.* and N. P. Suh†
University of South Carolina, Columbia, S.C.

The abrupt changes in the burning rate-pressure curve of M-2 double base propellant at low pressures were experimentally investigated and were found to be caused by the existence of a series of gas reactions in the "fizz" zone very near the solid-gas interface. The distance between these gas reactions and the solid-gas interface decreases with increase in pressure. The gas reaction zones are at temperatures higher than the surface temperature of the solid-gas interface. Using a model that assumes that the gas reactions only affect the heat transfer rate from the gas to the solid, the change in the burning rate of the propellant as a function of the initial temperature of the propellant was predicted. The agreement between the predictions of the theoretical model and the experimental results is good.

Nomenclature

A = area
c = specific heat of the solid propellant
d = distance from the solid-gas interface to regime R
E = activation energy
F = frequency factor
H = heat released by the reactions in the solid per unit volume
k = thermal conductivity of the solid propellant
m = reaction order
P = pressure
Q = heat transfer
R = universal gas constant
R_f = radiant flux
t = time
T = temperature
U = velocity of propagation of a regime of gas reactions
V = velocity of solid propellant (burning rate)
V_g = velocity of gas
W = constant of proportionality
Y = fraction of reactants available to react
Z = distance
α = parameter defined in text
β = radiation absorption coefficient
γ = dimensionless parameter defined in text
λ = parameter defined in text
ρ = density of solid propellant
τ = dimensionless time
Υ = parameter defined in the text

Subscripts

d = pressure coefficient
E = end
f = flux
g = gas
i = intercept
1 = for specified conditions
0 = initial
P = pressure
R = a regime
S = surface
T = total
v = volume

Received December 8, 1969; presented as Paper 70-124 at the AIAA 8th Aerospace Science Meeting, New York, January 19–21, 1970; revision received June 1, 1970. Supported by Picatinny Arsenal through the Army Research Office, Durham, Grant DA-ARO-D-31-214-61029.

* Post Doctoral Fellow. Associate Member AIAA.

† Associate Professor of Engineering; now, Associate Professor, Department of Mechanical Engineering, Massachusetts Institute of Technology, Cambridge, Mass.